THE THERMAL CONDUCTANCE OF URANIUM DIOXIDE/STAINLESS STEEL INTERFACES

A. C. RAPIER, T. M. JONES and J. E. McINTOSH

U.K.A.E.A., Reactor Development Laboratory, Windscale Works, Seascale, Cumberland

Abstract—The thermal conductance of uranium dioxide/stainless steel interfaces has been investigated in a disc-type apparatus under vacuum and with different interface gases (helium, argon, neon), and ranges of surface roughness ([11–1417] $\times$ 10^{-6} cm, arithmetical mean height measured from Talysurf profile records), interface gas pressure (7–1226 mm Hg), contact pressure (0–570 lb/in²), mean interface temperature (55–410°C), and heat flux (1–5·5 cal/s cm²). To obtain consistent results, the contact faces of the 2-cm diameter specimens were lapped optically flat and then roughened to a controlled amount. The thermal conductance is the sum of the solid conductance through the small areas of true contact, and the conductance through the gas in the interface (thermal radiation made a negligible contribution). The experimental values obtained for the solid conductance were of the same order as that predicted by the theory of Çetinkale and Fishenden. It was found, as expected, that the solid conductance between uranium dioxide and stainless steel was very low, owing to the hardness of the materials and the poor thermal conductivity of the uranium dioxide.

Predicted values of the gas conductance, based on several simple geometrical models of the roughness, and allowing for accommodation effects in collisions between the gas molecules and the surfaces, have been compared with the present experimental results and with other published data. In nearly all cases the measured conductance is within a factor two of the predicted value, which is considered to represent good agreement in view of the very wide range of variables covered by the data and the inaccuracies inherent in this type of measurement.

NOMENCLATURE

a, cross-sectional area;
b, peak-to-peak surface roughness;
c, wavelength of surface roughness;
d, effective fluid gap width;
f, fluid gap width;
g, temperature jump distance;
h, conductance/unit area;
k, thermal conductivity;
m, dimensionless parameter;
n, number of contact spots per unit area;
p, apparent contact pressure;
r, radius;
T, temperature;
u, conductance;
P, Prandtl number;
X, $b_t/2g$ ⎫
Y, b_t/d ⎬ dimensionless parameters;
Z, $\dfrac{4k_s b_t}{\pi k_f r_e}$ ⎭
α, accommodation coefficient of gas;
γ, ratio of specific heats of gas;

λ, mean free path of gas;
σ, yield stress.

Subscripts
1, 2, solids in contact;
m, harmonic mean;
c, contact;
$\left.\begin{matrix} d \\ e \end{matrix}\right\}$, with r defined in Fig. 4;
f, fluid;
s, solid;
t, total.

INTRODUCTION

ONE of the factors involved in predicting the performance of canned uranium dioxide fuel elements is the heat transfer coefficient between fuel and can, and the dependence of this coefficient on surface roughness, contact pressure, and interfacial gas. Theories have been put forward for estimating the value of the heat transfer coefficient across various interfaces

based on the thermal and physical properties of the materials involved, but few experimental data have been published for hard materials and poor thermal conductors such as uranium dioxide and stainless steel. It was therefore considered necessary to measure the heat transfer coefficient across stainless steel/uranium dioxide interfaces and to compare the results with theoretical predictions.

The subject of surfaces in contact has been extensively studied from a variety of points of view. The best overall reviews are by Holm [1] and by Bowden and Tabor [2]. A review of literature on heat transfer between metals in contact by Putnaerglis [3], whilst of limited value as an assessment of the state of knowledge, indicates the complexity of the problem and provides an extensive bibliography. Several workers have contributed to a theoretical analysis of the problem, in particular Çetinkale and Fishenden [4], Fenech and Rohsenow [5], and Laming [6], but their results are of limited application for reasons which will be discussed.

Qualitatively the mechanism of heat transfer is well understood. For relatively large conforming surfaces, such as two flat surfaces as used in the present investigation, the solids are only in contact at discrete points, and the total area of contact is only a small proportion of the total cross-sectional area, provided that the contact pressure is much smaller than the hardness. Over this contact area the full thermal and electrical conductivities of both materials are developed, and heat is transferred by solid conduction. Over the remaining area, heat is transferred by conduction in the fluid filling the space between the solids and by radiation, convection making a negligible contribution in practical cases. The contribution of radiation can be calculated in a straightforward manner, [4], and added to the calculated fluid and solid conductance. In most practical cases this contribution is negligible and will not be discussed further.

EXPERIMENTAL WORK

Description of apparatus

The general arrangement of the apparatus used in the investigation is shown in Fig. 1. It consisted of a central column, 2 cm in diameter, containing two uranium dioxide/stainless steel interfaces. An electrical resistance heater was housed in the top half of the central molybdenum rod, and heat flowed down the rod through the stainless steel disc (2 mm thick), the uranium dioxide disc (5 mm thick), the lower stainless steel disc (2 mm thick) and the copper rod which was water cooled. This column was surrounded by an outer guard ring assembly designed to eliminate radial heat losses. The outer guard ring consisted of two copper cylinders and a stainless steel cylinder, their thicknesses being adjusted to give a similar axial temperature gradient to that in the central column. The guard ring had its own resistance heater wound round the upper copper cylinder, and the power input to this heater could be varied independently of the central column heater. The voltage supplied to each heater was adjusted to a suitable value by means of variable output transformers from stabilized mains. The guard ring was surrounded by a shield, designed to minimize heat losses by convection and radiation, and the test apparatus was enclosed in a steel housing which could be evacuated or filled with any desired gas, water-cooled rubber sealing rings being used at the upper and lower flanges. Interface contact load was applied through a lever system sealed by a flexible bellows fitted on the top cover plate, and a Nimonic sphere. All thermocouple wires and heater supply leads were taken out of the apparatus through wax-filled gas seals.

The location of the chromel/alumel thermocouples (38 s.w.g. wires) used for measuring axial temperature gradients down the guard ring and central column assembly is indicated in Fig. 1. The molybdenum rod contained eight thermocouples positioned at 1-cm intervals $\frac{1}{2}$ cm deep, in a spiral down the axis of the rod. The upper and lower stainless steel discs contained two thermocouples each, positioned at the midplane, diametrically opposed, and the uranium dioxide sample contained four thermocouples positioned at 1-mm axial intervals in a spiral. The lower copper rod contained seven thermocouples positioned at 1-cm intervals in a spiral down the axis, and the outer guard ring contained a further nine thermocouples placed at suitable points in the copper and stainless steel cylinders.
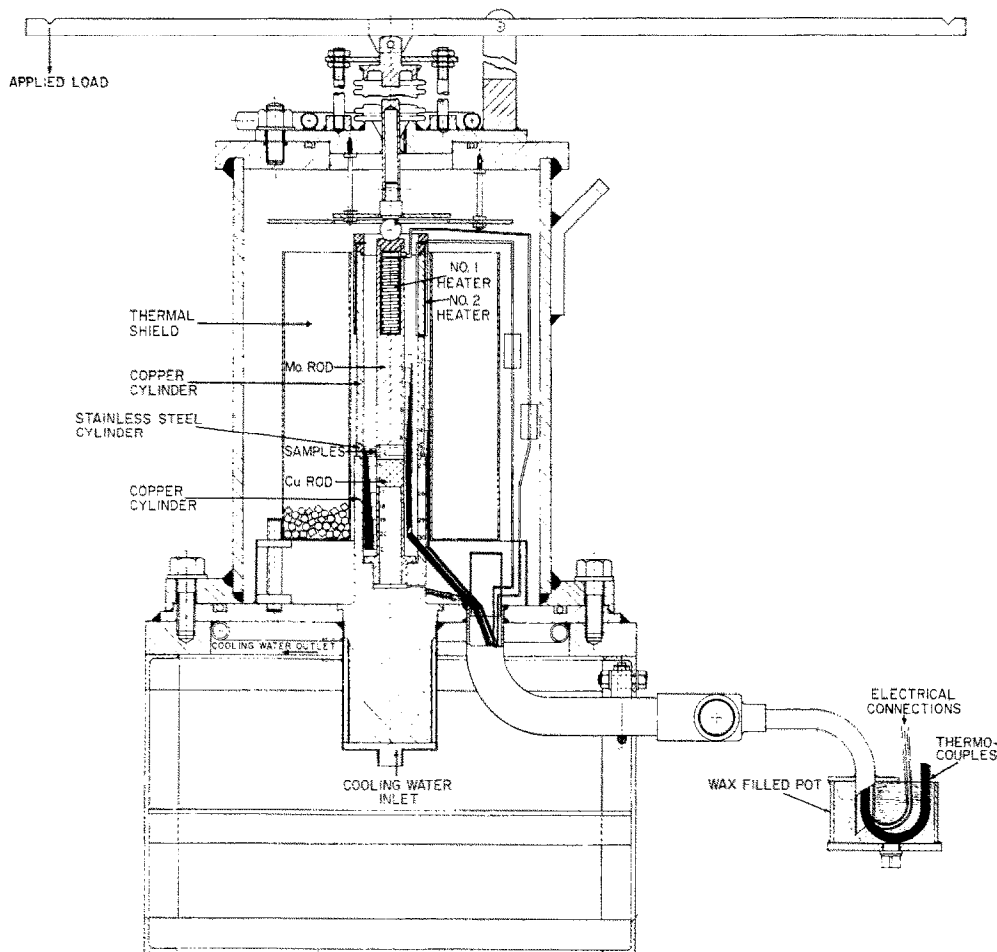
FIG. 1. Test apparatus.

Preparation of test specimens

Initial experiments carried out on surface-ground stainless steel and uranium dioxide samples resulted in large differences in the temperatures indicated by the two diametrically opposed thermocouples in the stainless steel discs, and in very uneven temperature distribution down the uranium dioxide disc. These observations were attributed to non-uniform heat flux distributions at the interfaces caused by the surfaces having deviations from flatness, which were large compared with the surface roughness, resulting in contact over only limited areas. Previous results could not be repeated when the same specimens were re-assembled, and the influence of changes in surface roughness

and other factors could not be resolved. To overcome these difficulties the contact surfaces were first lapped to optical flatness, within one light wavelength ($11 \cdot 6 \times 10^{-6}$ in), and then roughened to a controlled degree. The different surface finishes were obtained with the following abrasives:

Uranium dioxide: 120 Carborundum, 1F Carborundum, 3-micron diamond, polished.

Stainless steel: 120 Carborundum, 302 emery, 3-micron diamond, polished.

Some of the surface finishes obtained by these abrasives are illustrated in Fig. 2, and the surface roughness of each sample is given in Table 1, the traces being obtained with a
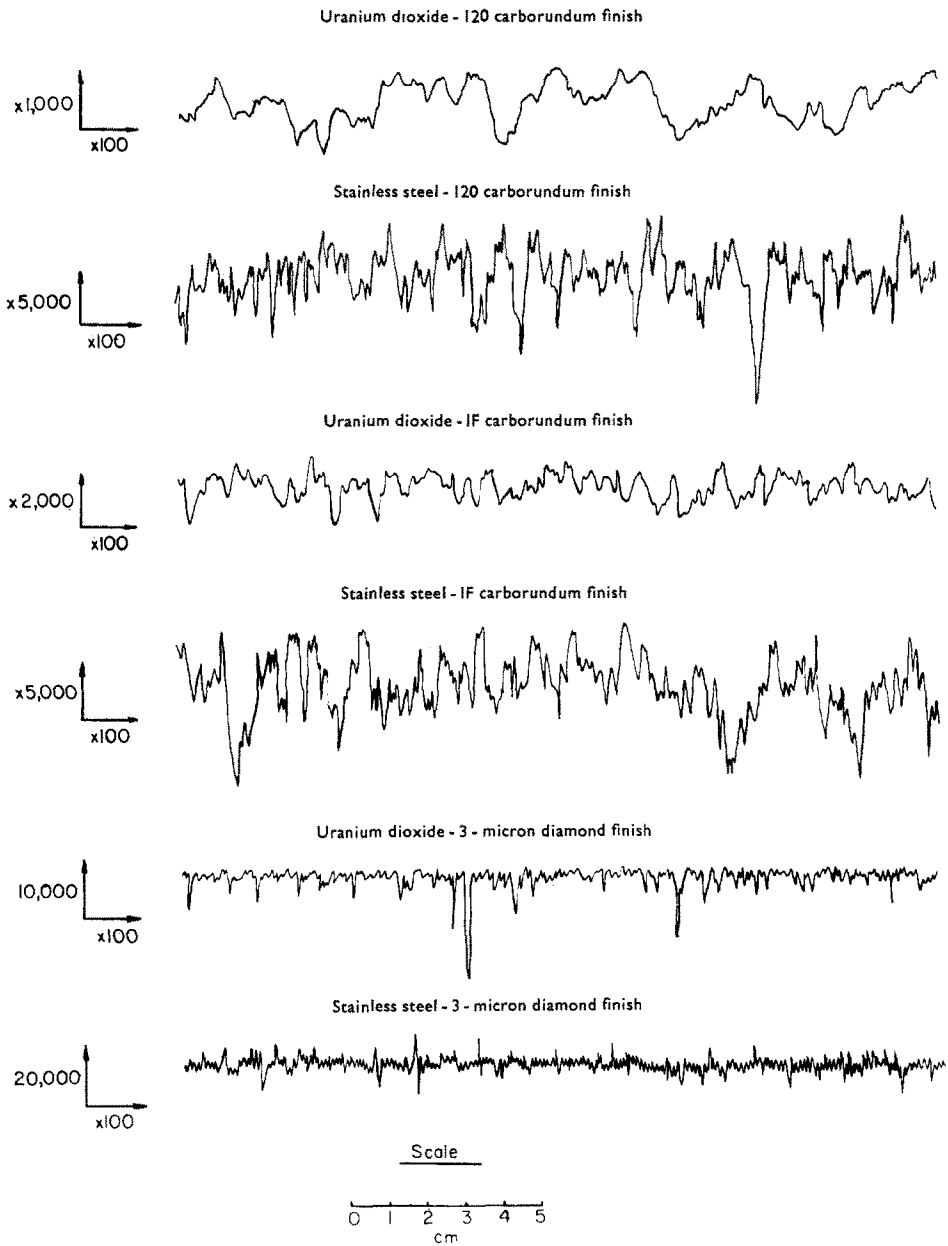
FIG. 2. Typical surface profiles of the samples.

Table 1. *Test programme showing combination of surfaces and interfacial gases*

No.	Uranium dioxide			Stainless steel			Vacuum 10^{-3} mm Hg	Argon	Helium	Neon
	Surface	b_1, cm	c_1, cm	Surface	b_2, cm	c_2, cm				
1	120 Carborundum	1386×10^{-6}	$1 \cdot 53 \times 10^{-1}$	120 Carborundum	942×10^{-6}	$0 \cdot 79 \times 10^{-1}$	×	×	—	—
2	120 Carborundum	1386	1·53	3-micron diamond	50	0·13	×	×	×	—
3	120 Carborundum	1386	1·53	302 emery	356	0·37	×	—	—	—
4	3-micron diamond	40	0·16	302 emery	356	0·37	×	×	×	—
5	1F Carborundum	614	0·4	120 Carborundum	942	0·79	×	×	×	—
6	1F Carborundum	614	0·4	3-micron diamond	50	0·13	×	×	×	—
7	Polished	16	0·18	Polished	6	0·1	×	×	—	×
8	120 Carborundum	2000	1·21	120 Carborundum	834	0·60	×	×	×	×
9	120 Carborundum	2000	1·21	302 emery	356	0·37	×	×	×	×

× = tested

Talysurf surface analyser. Each surface was thoroughly cleaned before assembly, and care was taken to ensure that no loose grit or dirt got into the interface during assembly of the apparatus.

Test procedure

When the apparatus had been assembled with a selected combination of surface finishes on the stainless steel and uranium dioxide discs, a known contact pressure was applied to the central column and the chamber was evacuated. Power was applied to the guard ring and central column heaters, and a constant flow of cooling water passed over the lower copper rod. The assembly usually took 2–3 h to attain steady temperature conditions, but intermediate temperature checks were taken during this period, and if the guard ring temperatures differed from the corresponding temperatures down the central column, the power input to the guard ring could be adjusted accordingly. When steady state conditions had been attained the temperature readings at all points were measured by means of a potentiometric indicator. The procedure was repeated for other values of the power input; a typical set of test results is shown in Fig. 3.

From the known thermal conductivity values of molybdenum and copper at the appropriate temperatures, and the associated temperature gradients, the heat fluxes down both rods could be calculated. For the range of tests covered, these calculated heat fluxes agreed to within 5–10 per cent, and indicate the effectiveness of the guard ring assembly in minimizing radial heat losses. Once the thickness of the copper and stainless steel cylinders forming the guard ring had been established during preliminary test

runs, no trouble was experienced in obtaining the required temperature levels by adjusting the power input to the heater. Some typical guard ring temperature distributions are included in Fig. 3.

The calculated heat flux down the molybdenum rod was used to obtain the temperature gradient down the stainless steel discs, and from the known centre temperatures of the steel discs the temperature at the contact surfaces could be determined. From the temperatures at four positions in the uranium dioxide disc the temperatures at the surfaces were obtained by extrapolation of the linear gradient. Hence the temperature drop at each interface was determined, and the heat transfer coefficient or thermal conductance at the interface could then be calculated. The procedure was repeated for a range of values of power input, and with helium, argon or neon gas filling the test chamber.

Nine combinations of surface roughnesses were investigated (see Table 1) the arithmetical mean height of the surfaces measured from Talysurf profile records ranging between 11×10^{-6} and 1417×10^{-6} cm.

The effects of three interface gases (helium, argon and neon) were investigated as well as vacuum, the gas pressures ranging between 7 and 1226 mm Hg.

Interface contact pressure ranged between 0 and 570 lb/in², and the heat fluxes ranged between 1 and 5·5 cal/s cm², the mean interface temperature ranging between 55°C at the lower interface and 410°C at the upper interface. The maximum value of heat flux, and hence interface temperature, was governed by the maximum operating temperature of the electrical heater windings.
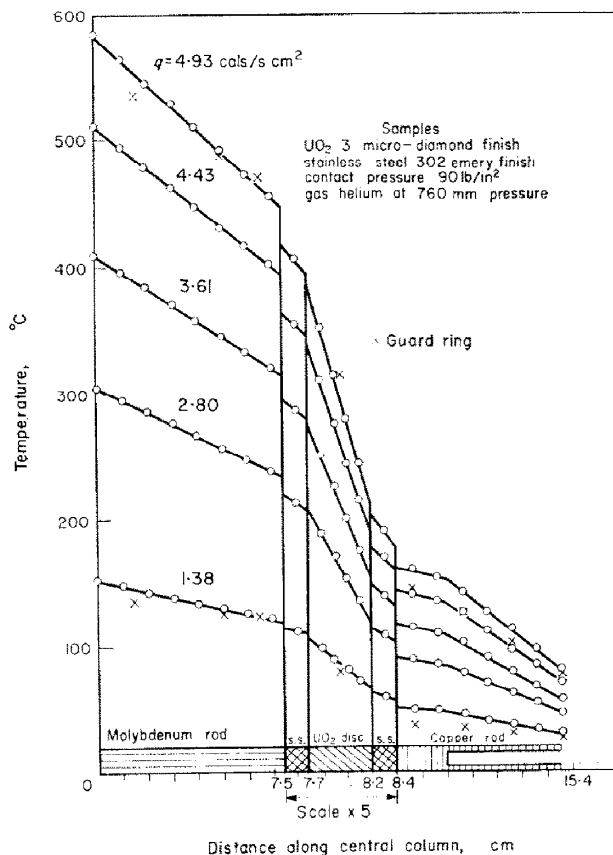
FIG. 3. Typical temperature distribution.

Accuracy of test results

The thermal conductance of an interface is derived from the estimated heat flux and temperature difference across the interface, and the accuracy of these measurements in the present investigation will now be briefly discussed.

A statistical analysis was carried out on a random selection of test results, and showed that for 95 per cent confidence limits the surface temperatures of the uranium dioxide samples, estimated by extrapolation of the gradient in the sample, were accurate to ±2·7 degC. Similarly, the surface temperatures of the stainless steel discs were accurate to ±1·8 degC and the temperature differences at the interfaces were therefore accurate to ±3·2 degC. This is large compared with the measured temperature differences with helium as the interfacial gas, and accounts for the scatter in results at low heat fluxes.

In calculating the heat fluxes down the molybdenum and copper rods, the thermal conductivities at the appropriate temperature were assumed to be accurate to ±5 per cent, and analysis of the temperature gradients down the molybdenum and copper rods showed that these were accurate to ±4·80 and ±4·97 per cent respectively. The estimated accuracy of the heat flux values is therefore approximately ±7 per cent, and as previously mentioned the agreement obtained between the calculated heat fluxes down the molybdenum and copper rods was within these limits.

THEORETICAL TREATMENT

Surface contact

When two surfaces are brought together, they come into contact at only a number of discrete points. The distribution of these points of contact clearly depends on both the accuracy to which the surfaces have the same overall geometry and the type of surface roughness. The following discussion is confined to surfaces which, over the contact area considered, conform to each other to an accuracy of a small proportion of the larger peak-to-trough roughness. In practice this is achieved by either machining the surfaces to the same shape or making one of the surfaces sufficiently flexible and deforming it into contact by pressure. It is in fact difficult to achieve this uniformity of contacts unless very special precautions are taken. Ordinary machine tools do not produce surfaces geometrically accurate to the same order as the surface roughness. Although a surface may be flexible enough to deform into contact over the area in general, it may still be stiff enough to form "bridges" large compared with the roughness. This is a serious limitation of much experimental work and will be discussed later. Many parameters are required to completely specify the roughness of a surface. The surface is examined by taking profiles in various directions across it. The usual parameter quoted is either the average or the r.m.s. value about the mean line, but for the thermal conductance we are interested in the average wavelength, or spacing between the major peaks on the surface, c, and the mean height between major peaks and troughs, b. Usually c is of the order of $10b$. Most surfaces in practice are ridged, i.e. c varies with the direction in which the traverse is taken.

Solid conductance

Solid conductance is the sum of the conductances of all the contact spots. Meaningful experimental results will only be obtained if the contact spots are all of the same order of size, and uniformly distributed over the area investigated. The number of points of contact and their distribution has been discussed in detail [1–6]. In most experimental work, the roughness has been produced by machining either regular ridges [4–6] or pyramids [5] on

flat surfaces. For artificial pyramids in contact with a flat surface, the number of contact spots per unit area, n, is defined. For systematic ridges, Laming [6] used

$$n = \frac{\sin \varphi}{c_1 c_2} \qquad (1)$$

where φ is the angle between the direction of the ridges, but found that φ has little effect. The probable explanation of this is that the crests of the ridges on the rougher surface have irregularities of the same order of size as the irregularities on the smoother surface. Since no special precautions were taken about the flatness of the surfaces these results are suspect, particularly at low contact pressures. Fenech and Rohsenow [5] use the surface profiles to determine n for various amounts of overlap, but do not take changes in profile due to the deformation of the peaks into account.

In the present work, the roughnesses investigated are isotropic, i.e. they show no systematic variation of profile with direction and are of relatively small height. With the careful method of surface preparation and relatively low contact pressures used, the number of contact spots is determined by the peaks on the rougher surfaces.

A line traverse of this surface is unlikely to include a peak, but it will include a major undulation for every peak inside a strip of width $2r_e$, where r_e is the average "equivalent" radius associated with each contact spot (Fig. 4) given by

$$n = \frac{1}{\pi r_e^2}$$

∴ number of peaks/unit length of traverse

$$= \frac{1}{C_1} = 2r_e n$$

$$\therefore n = \frac{\pi}{4C_1^2}. \qquad (2)$$

Small undulations will tend to be neglected and this estimate of n will only be approximate.

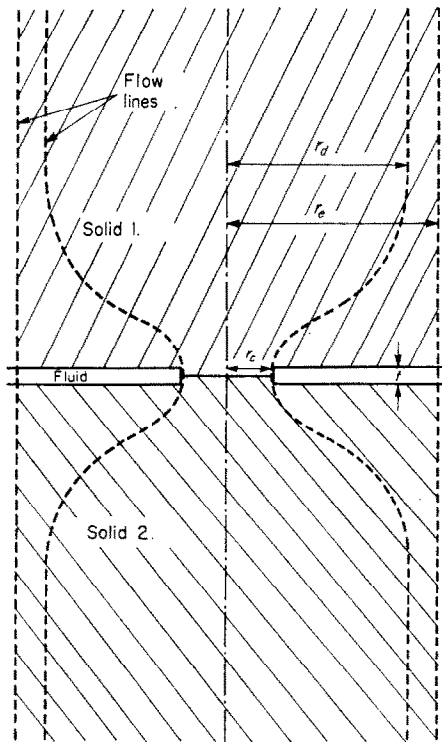When an apparent contact pressure p is applied to the interface, the area in the softer

FIG. 4. Idealized contact spot.

material around each contact spot is plastically deformed until

$$\frac{\text{contact area}}{\text{total area}} = \frac{r_c^2}{r_e^2} = \frac{\text{apparent pressure } p}{\text{indentation hardness}}. \quad (3)$$

This enables the average radius of a contact spot, r_c, to be estimated if the indentation hardness is known. The choice of the value of indentation hardness to use is discussed in the Appendix.

The heat flowing through the area radius r_c is drawn from a cylinder radius r_d in the body of the material (Fig. 4). This constriction of the heat flow gives rise to an additional temperature drop in the solid. It is a standard result, discussed in detail by Holm [1] and reproduced by Çetinkale and Fishenden [4], that this constriction effect can be expressed as

conductance of one spot u

$$= \frac{\text{heat flux}}{\text{additional temperature drop}}$$

$$= \frac{2\pi r_c k_s}{\tan^{-1}[(r_d - r_c)r_c]} \quad (4)$$

$$\rightarrow 4r_c k_s \text{ for } r_d \gg r_c. \quad (5)$$

If there is a temperature drop on each side of the spot in materials of conductivities k_{s1} and k_{s2} and

$$\frac{2}{k_{sm}} = \frac{1}{k_{s1}} + \frac{1}{k_{s2}} \quad (6)$$

then

$$u = \frac{\pi r_c k_{sm}}{\tan^{-1}[(r_d - r_c)r_c]}. \quad (7)$$

It follows from equations (2), (3) and (7) that

conductance/unit area $= h_s = un$

$$\frac{\dfrac{\pi}{2} \dfrac{k_{sm}}{c_1} \sqrt{\left(\dfrac{p}{\text{indentation hardness}}\right)}}{\tan^{-1} \dfrac{r_d - r_c}{r_c}} \quad (8)$$

$$\rightarrow \frac{k_{sm}}{c_1} \sqrt{\left(\frac{p}{\text{indentation hardness}}\right)}, r_d \gg r_c.$$

Fluid conductance

In calculating fluid conductance, three factors have to be taken into account: (a) the "accommodation" effect of gas molecules contacting a surface at a different temperature, and only acquiring part of the temperature difference, (b) free molecule conductance when the gap becomes of the same order of size as the mean free path of the molecules, (c) non-uniformity of the gap.

The first two effects are fully discussed by Kennard [8]. Firstly he shows that the accommodation effect can be considered as increasing the gas conduction path at each surface by a "temperature jump distance" g given in terms of the mean free path of the gas λ by his equation (238b) which may be rewritten

$$\frac{g}{\lambda} = \frac{2}{P} \times \frac{2 - a}{a} \times \frac{\gamma}{\gamma + 1} \quad (9)$$

where P is the Prandtl number, a is the accommodation coefficient, γ is the ratio of specific heats.

Secondly he considers the case when collisions between molecules can be neglected. When the accommodation coefficient is the same at both
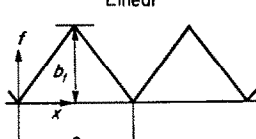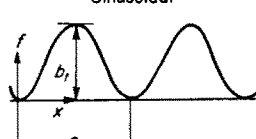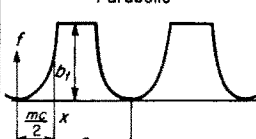
Idealized gap distribution	Linear	Sinusoidal	Parabolic
Method of calculation of effective gap	$\dfrac{f}{b_r} = \dfrac{2x}{c}$, $0 < x < \dfrac{c}{2}$ $= 2 - \dfrac{2x}{c}$, $\dfrac{c}{2} < x < c$	$\dfrac{f}{b_r} = \dfrac{1}{2}\left[1 + \sin\dfrac{\pi}{2}\left(\dfrac{4x}{c} - 1\right)\right]$	$\dfrac{f}{b_r} = \left(\dfrac{2x}{mc}\right)^2$, $-\dfrac{mc}{2} < x < \dfrac{mc}{2}$ $= 1, \dfrac{mc}{2} < x < c\left(1 - \dfrac{m}{2}\right)$
Arithmetic mean $d = \dfrac{\int f dx}{\int dx} + 2g$	$\dfrac{1}{\dfrac{1}{2} + \dfrac{1}{X}}$	$\dfrac{1}{\dfrac{1}{2} + \dfrac{1}{X}}$	$\dfrac{1}{1 - \dfrac{2}{3}m + \dfrac{1}{X}}$
Volumetric mean $d = \dfrac{\int f d\sigma}{\int d\sigma} + 2g$	$\dfrac{1}{\dfrac{2}{3} + \dfrac{1}{X}}$	$\dfrac{1}{\dfrac{1}{2} + \dfrac{2}{\pi^2} + \dfrac{1}{X}}$	$\dfrac{1}{1 - \dfrac{m^2}{2} + \dfrac{1}{X}}$
a.r.m.r. $d = \dfrac{\int dx}{\int \dfrac{dx}{f+2g}}$	$\log_e(1+X)$	$\dfrac{X}{\sqrt{1+X}}$	$\dfrac{1-m}{1+\dfrac{1}{X}} + m\sqrt{X}\tan^{-1}\sqrt{X}$
v.r.m.r. $d = \dfrac{\int d\sigma}{\int \dfrac{d\sigma}{f+2g}}$	$2\left[1 - \dfrac{1}{X}\log_e(1+X)\right]$	——	$\dfrac{1-m^2}{1+\dfrac{1}{X}} + m^2\log_e(1+X)$

FIG. 5. Idealized surface profiles.

surfaces it can be shown, from his equations (242a, b, c), that the effective width of gap of gas of normal conductivity is $2g$ where g is again given in terms of λ by equation (9). The values of λ and conductivity used must be those determining the diffusion of molecules into the gap. When the gap is sufficiently small over only a small proportion of the total contact area, it is the conditions in the adjacent wider sections that are relevant. If however the gap is small everywhere, it is the conditions outside the gap that must be used. In the present experimental work, the guard heater arrangement ensures that conditions immediately outside the gap are similar to those inside.

The type of non-uniformity of gap width to be expected can be seen from the typical surface profiles in Fig. 2. For the purpose of calculating this effect, several idealized variations of total gap-width f with traverse direction x have been assumed. These are shown in Fig. 5. f varies from zero at the contact points spaced at intervals c to a maximum of $b_t = b_1 + b_2$ where b is the mean change in height between the main peaks and troughs on the surface profile.

At any point the effective gap width is $f + 2g$ assuming the same accommodation coefficient at each surface. A mean effective gap d can be defined in two ways: firstly as the simple average of $f + 2g$, or secondly, since the local conductance is proportional to the reciprocal of the local gap and the sum of these conductances in parallel is required, as the reciprocal mean reciprocal (r.m.r.) value. Two types of surface have been considered, firstly ridges having idealized profiles in a direction perpendicular to the ridges, "arithmetic means", and secondly surfaces having gaps with radial symmetry about the contact points, "volumetric means", e.g. the volumetric mean for a linear variation of f corresponds to contact points which are cones (the solution for pyramids is exactly the same).
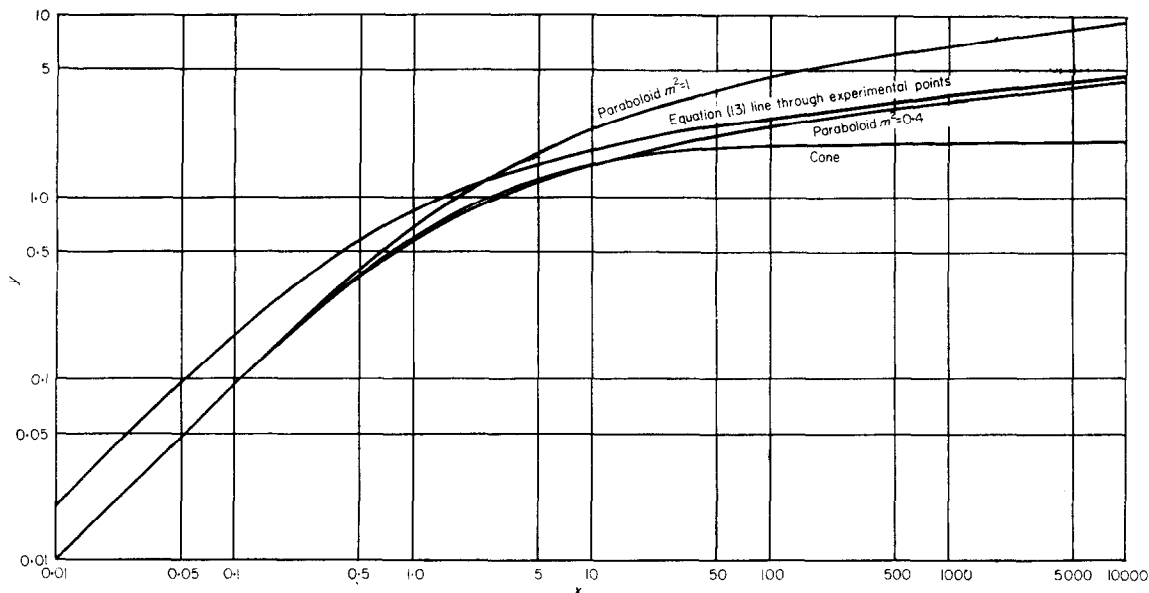
FIG. 6. Theoretical variation of Y with X.

The expressions for d in terms of g and b_t, or more conveniently, $Y = b_t/d$ in terms of $X = b_t/2g$ are summarized in Fig. 5 and some v.r.m.r. values are plotted in Fig. 6. As would be expected all the cases give $Y \to X$ for small values of X, i.e. $d \to 2g$. For larger values of X, the small gaps near the contact points become dominant in calculating r.m.r. values. No simple expression was found for the v.r.m.r. for the sinusoidal profile but it should, under these conditions, be close to the value for the parabolic profile of the same radius of curvature contact, i.e. $m = 2/\pi$ (the a.r.m.r. expressions tend to the same limit for this value of m) or $m^2 \simeq 0.4$. It was checked by numerical methods that this is the case.

It has been assumed in these calculations that the area of solid contact is negligible, and that each solid surface is at a constant temperature. As a result of this, some solutions predict that Y increases indefinitely with increasing X, but this requires a large concentration of heat flux round the contact points and additional temperature drops due to the constriction effect. This is a complicated problem to solve exactly, but an estimate of the magnitude of this effect can be obtained by assuming that solid conductance is dominant inside a radius r'_c

defined as the radius at which the average conductance due to the constriction effects equals the conductance due to the local gas gap. The two analytical expressions for v.r.m.r. (Fig. 5) modified in this way for large values of X give:

(a) *Cones*

$Y \to 2$, as before, together with

$$\frac{\text{temperature drop across fluid in interface}}{\text{additional temperature drop in solid on one side due to constriction effect}} = Z = \frac{4}{\pi} \frac{k_s}{k_f} \frac{b_t}{r_e}. \quad (10)$$

(b) *Paraboloids*

$$Y \to 1 + 2m^2 \log_e \frac{Z}{m}. \quad (11)$$

For many combinations of solids and gases found in practice Z is of the order of 10, corresponding to an upper limit for Y of 3·2 for $m^2 = 0.4$. This limit is insensitive to the value of Z used.

CORRELATION OF EXPERIMENTAL RESULTS
Solid conductance

Tests under vacuum to determine the solid conductance were carried out with contact

pressures between zero and 570 lb/in². The results were independent of heat flux and interface temperature to the accuracy of the experiment. There was a general increase of conductance with increase of contact pressure, but the variation was not as great as predicted theoretically. There are several possible reasons for this. The maximum contact pressure available, whilst representative of the pressures of practical interest, is very small compared with the hardness of the materials used. The method of preparation of the specimens results in the tips of the peaks being sections of the original optical flats. At low loads, therefore, the effective value of c may be much smaller than the value estimated from the surface profiles. The gradual increase in the effective value of c with increase in pressure could account for the variation of conductance being smaller than predicted. The method used to apply the load did not ensure that its line of action passed through the centre of the specimens, and the contact pressure may not be uniform. This was certainly true at very low loads, when the results were not very consistent. A constant

pressure of 91 lb/in² was used for most of the tests, to ensure that a consistent and reproducible value of solid conductance was maintained whilst the fluid conductance was investigated.

Putting the following values into equation (8),

p = 91 lb/in²
indentation hardness of stainless steel
$$= 6 \times 10^5 \text{ lb/in}^2$$
k_{s1} = 0·015 cal/s cm degC for uranium dioxide
k_{s2} = 0·040 cal/s cm degC for stainless steel
k_{sm} = 0·022 cal/s cm degC

we have

$$h_s \simeq \frac{3 \times 10^{-4}}{\text{larger } c} \text{ cal/cm}^2 \text{ s degC.}$$

This equation is plotted in Fig. 7 as contours of h_s on a graph of the wavelength for the uranium dioxide surface against the wavelength for the stainless steel surface with the experimental results of Table 2 superimposed. The biggest discrepancies between the theoretical predictions and experimental results occur when one of the contact surfaces is polished stainless steel. Under
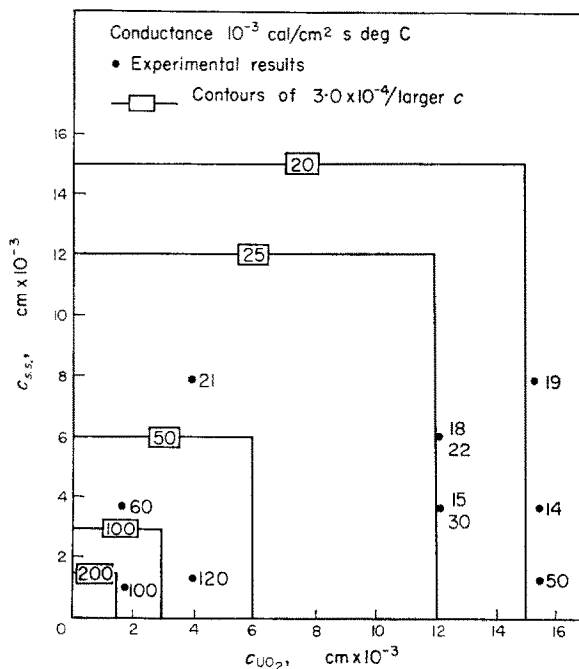

FIG. 7. Solid conductance results.

these conditions the sections of the original optical flats on the uranium dioxide will contact an optically flat steel surface giving a higher conductance than predicted. For "hard" materials, solid conductance usually only contributes a small proportion of the total conductance, and it was not the object of the present investigation to determine this accurately.

Fluid conductance

The fluid conductance was obtained by subtracting the solid conductance, the conductance of the same surface combination in vacuum, from the total conductance. The effective gap was calculated as the thermal conductivity of the fluid at the interface temperature, divided by the fluid conductance:

$$d = \frac{k_f}{h_f}. \qquad (12)$$

Values of accommodation length g were calculated from Table 3, assuming that the mean free path is proportional to the absolute temperature divided by the gas pressure. The peak-to-trough roughness of a surface was taken as twice the arithmetical mean roughness, as measured with a Talysurf. The peak-to-peak roughness of the combination of surfaces was taken as the sum of the peak-to-trough roughness of the two surfaces.

X and Y were calculated for each experimental result* and plotted in Fig. 8. Also shown on this figure is the expression:

$$Y = \frac{0 \cdot 6}{1 + (1/2X)} + 0 \cdot 4 \log_e (1 + 2X). \qquad (13)$$

This is the result predicted for paraboloids with $m^2 = 0 \cdot 4$ but with X multiplied by a factor two. It is seen to be a good representation of the experimental results. The results for a particular combination of surfaces are shown separately in Fig. 9. The correlation between different gases is seen to be very good, suggesting that the method of correlation and values of accommodation coefficient used are appropriate. A wide range of accommodation coefficients is sometimes quoted, particularly for helium, but usually the values which differ substantially from those in Table 3 have been found at specially prepared surfaces.

There are several possible explanations of the fact that the experimental values would have agreed well with theory if X had been found to be twice as large. Firstly the temperature jump distance could be over-estimated by equation (9). It is very difficult to measure this distance by direct experiment to check the theory. It was

---

* A table giving detailed results of 200 tests may be obtained from the authors.

Table 2. Solid conductance with 91 in² contact pressure

Surface combination (see Table 1)	1	2	3	4	5	6	7	8a	8b	9a	9b
Thermal conductance cal/cm² s degC × 10⁻³	19	50	14	60	21	120	100	18	22	15	30

Table 3. Gas properties

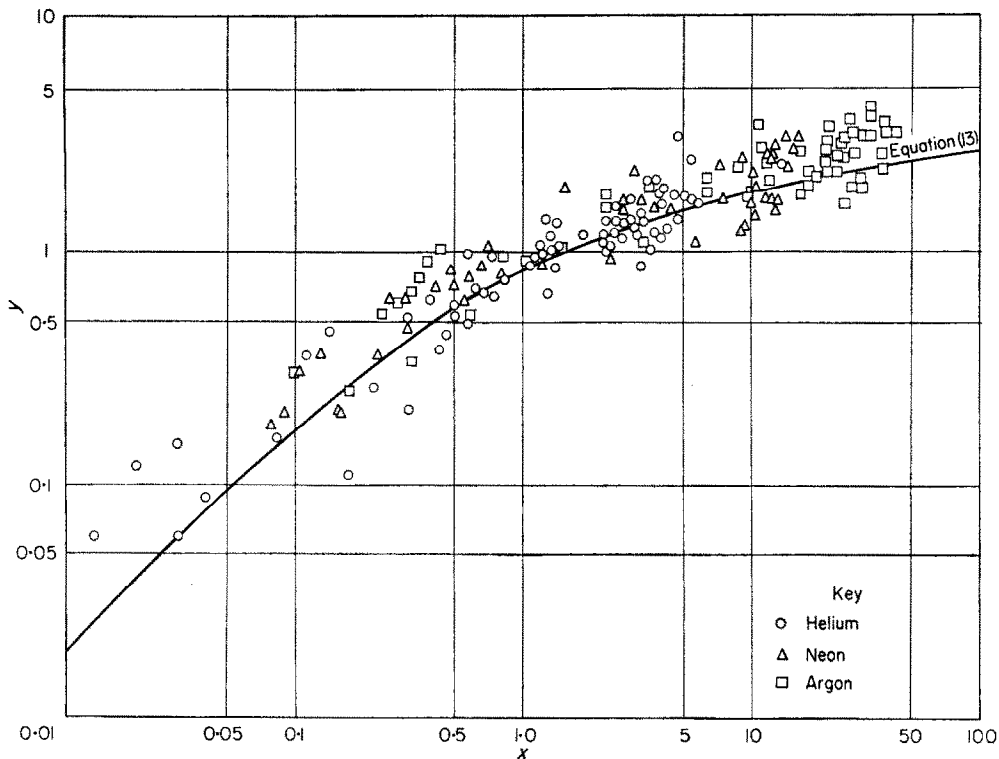| Gas	γ	P at 300°C	a (International Critical Tables)	$\frac{2g}{\lambda}$	λ at n.t.p. (cm × 10⁻⁶)
Helium	1·667	0·72	0·38	14·8	28·5
Neon	1·667	0·70	0·65	7·4	19·5
Argon	1·667	0·67	0·85	5·10	10·0
Air	1·403	0·71	0·83	4·6	9·6
Hydrogen	1·41	0·71	0·26	22·1	16·0

FIG. 8. Gaseous conductance results.

stated in the previous section that appropriate temperature and pressure values to use in calculating g tend to be those in the pressure vessel rather than in the gap when λ becomes large, i.e. particularly for helium at low pressures. This could increase X by a factor of two in the worst case. Secondly, the peak-to-trough roughness may have been under-estimated by the assumptions made. Thirdly, with the method used to prepare the surfaces, parts of the original optical flats will exist near the contact points, making the proportion of relatively small gap greater than is assumed for the idealized surfaces.

GENERAL DISCUSSION AND COMPARISON WITH PREVIOUS WORK

Solid conductance

The theoretical derivation of the conductance of a single contact spot gives the result expressed in equation (4), and this would appear to be sufficiently accurate for most purposes. Two attempts have, however, been made to confirm the theoretical predictions. Firstly Çetinkale and Fishenden [4] have used relaxation methods to solve this problem and shown that their results are in good agreement with equation (4). Secondly Fenech and Rohsenow [5] have carried out experiments on large-scale models of the idealized contact spot (Fig. 4) with various fluids in the gap. It is possible to predict the results for each of their experiments by finding a value of r_d by trial and error such that the temperature drop across the fluid is the same as the temperature drop due to the constriction effect in the metal on each side of the junction plus the temperature drop in the metal column forming the spot. Such predictions are in much better general agreement with the experimental results than the predictions of Fenech and Rohsenow's much more complicated theory. The use of equation (4) would seem therefore to be justified. The "alleviation effect", the increase in conduc-
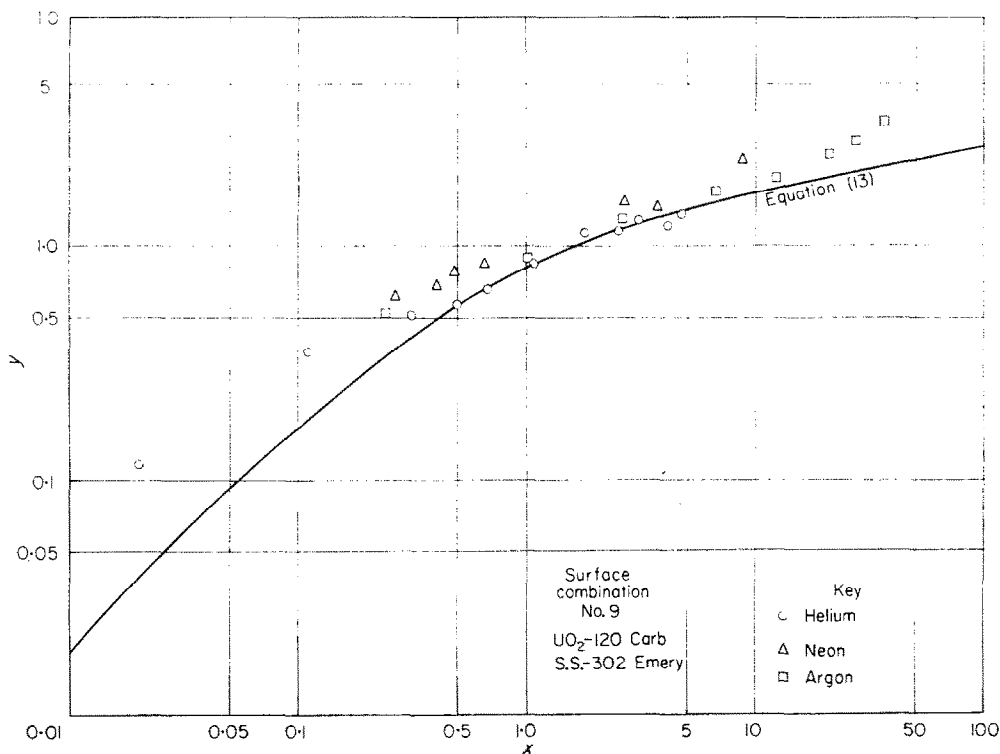
2D

FIG. 9. Gaseous conductance results for a particular surface combination.

tance due to adjacent spots, is found by dividing equation (4) by equation (5) giving

$$1 \left/ \frac{2}{\pi} \tan^{-1} \frac{r_d - r_c}{r_c} \right. .$$

For most practical cases this can be taken as 1 but it is sometimes necessary to apply this correction. Laming [6] uses a different correction due to Roess which seriously over-estimates this effect.

In most experimental work on solid conductance no special precautions have been taken to ensure uniformity of engagement of the contact surfaces, and agreement with theory for the variation of conductance with contact pressure is poor.

Fenech and Rohsenow [5] give results of the variation of h with p which on logarithmetic scales give a slope of $1/2$ for low p, increasing to 1 for large p. They explain this result by a very large increase in the number of contact spots as p is increased, but the same effect would be produced by a decrease in hardness. This is more consistent with the fact that they were able to reproduce this result on repeated loading, since the variation of number of contact points with load would not be expected to be the same before and after plastic deformation.

Laming [6] produces results which differ from predictions in several respects, and explains the discrepancies by the high hardness observed with very small point loads. He uses, as a justification for his choice of fluid conductance value, the fact that the remaining solid conductance varies linearly with load on logarithmic scales, with a slope of about $3/4$ and not $1/2$ as predicted by theory. A relatively small change in the value of fluid conductance could alter this slope appreciably at the lower loads. He dismisses the idea of the number of contact spots increasing with load on the grounds that the slope should decrease with increasing load if this were happening. If, however, there is a work-hardened layer or high microhardness, it could hide this effect. For his

finest surfaces, flatness correct to a few micro-inches, which can only be achieved by optical manufacturing techniques, would be required for engagement to be complete at relatively low loads. At higher pressures the slope becomes 3/4, after using the correction due to Roess discussed above, and it is the difference of this value from 1/2 that leads to the predicted variation of hardness with load per spot. At these higher loads a correction for the effective reduction in hardness as the contact spots became close together could appreciably alter this slope and conclusion. It is impossible to separate all these effects. Although there is some evidence for increase in hardness with decrease of load per spot, very small changes in the assumptions made in the calculations could eliminate the need for postulating "fabulously high" values.

Cohen, Lustman and Eichenberg [10] measured the conductance between a uranium dioxide pellet and a thick steel cylinder. The contact pressure is deduced from the differential expansion of the pellet and the cylinder. A very rapid increase in conductance is observed at a contact pressure very much lower than the hardness value. The reasons for this are discussed in the Appendix.

The theoretical estimate of the solid conductance per unit area of an interface is given by equation (8). There is no satisfactory experimental confirmation of this estimate, although very approximate agreement has been shown for some cases. The most important reason for this is the difficulty in determining the value of two of the parameters applicable under the experimental conditions. Firstly, under some conditions, the appropriate indentation hardness will not be the value normally measured, as discussed in Appendix I. Secondly, it is difficult to determine the true mean value of the pitch of the contact spots, c_1, from examination of surface profiles. Also in most work, no precautions were taken to ensure that the surfaces were geometrically accurate enough for contact to occur at all the roughness peaks, particularly at relatively low contact pressures.

There is still scope for an investigation using carefully prepared specimens, under vacuum, over a wide range of contact pressures, to provide experimental confirmation of the theoretical predictions of solid conductance. The difficulties of experimentally determining conductance could equally well be put as difficulties of estimating it for practical cases.

Fluid conductance

Experimental results for gaseous conductance have been taken from various references, and are shown plotted as Y against X in Fig. 10. Some authors have quoted values of gaseous conductance, but where this has not been done values have been deduced, usually by extrapolation to zero contact pressure of the variation of conductance with contact pressure. Çetinkale and Fishenden [4, 9] deduce the correlation equivalent to

$$Y = \frac{1}{0 \cdot 305 + 1/X}$$

which is effectively the arithmetic mean value with a different numerical constant. Their experimental results were for large values of X, and in fact only confirm that $Y \simeq 1/0 \cdot 305$ in this region.

An analysis by Fenech and Rohsenow [5] concludes that

$$Y = 5 \cdot 8 \frac{\text{maximum gap}}{\text{volumetric average gap}} - 4 \cdot 8.$$

The accommodation effect is not considered. One of their experimental points, $Y = 1 \cdot 6$, $X = 1660$, is deduced from tests with artificial pyramids on an optical flat, and is in good agreement with the prediction of Y slightly less than 2 for this arrangement. Laming's [6] conclusion is that $Y = 3$.

Cohen, Lustman and Eichenberg [10] measure the "effective" conductivity of a uranium dioxide cylinder and its surrounding gas gap when enclosed in a thick-walled steel cylinder and heated by nuclear irradiation. In order to calculate the gap conductance, assumptions have to be made about the conductivity of the uranium dioxide. The mean gap under operating conditions is calculated from the initial gap and the expansions of the components. They conclude that the properties of the gas in the gap do not influence the gap conductance. They attempt to explain this by large variations in the
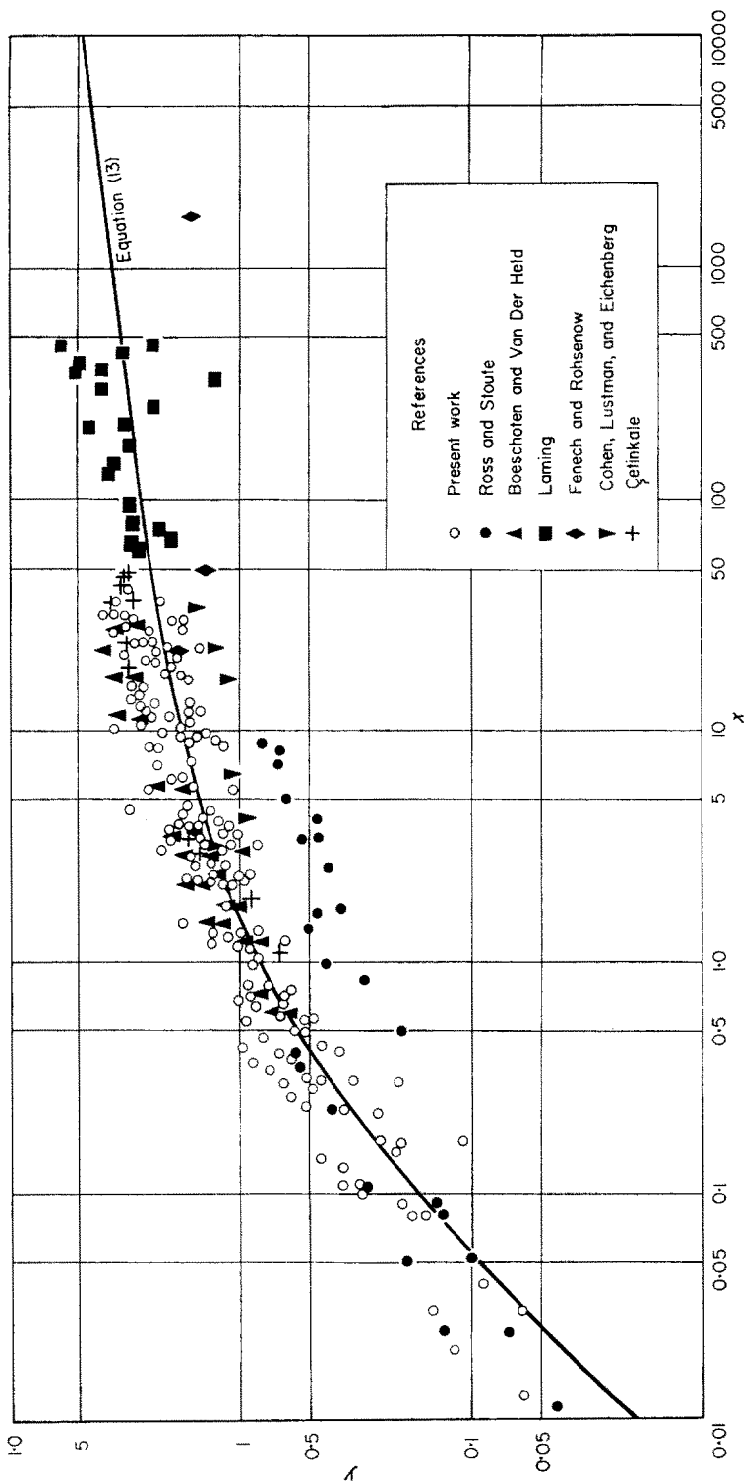
FIG. 10. General correlation of gaseous conductance results.

accommodation coefficients of some gases, but, as can be seen from Fig. 10, most of their results are for values of X where this is unimportant. They discuss a different derivation of the accommodation effect. However if equation (9) and the values in Table 3 are used to recalculate their Fig. 16, almost exact agreement is obtained with their theoretical predictions. A possible reason for their anomalous experimental results is that the uranium dioxide does not remain central in the steel cylinder, but touches it at one side. Predictions of gap conductance on this assumption are much closer to the observed values, and the predicted effect of gas properties is much smaller. A second possible reason is that, unless special precautions have been taken to clean and de-gas both can and fuel before assembly, relatively large quantities of gas will be evolved on heating, possibly forming the bulk of the interface gas in every case. It must also be remembered that this particular experiment is not at all an accurate method of determining gap conductance.

Ross and Stoute [11] have measured the conductance between zircaloy and uranium dioxide for the gases helium, argon, krypton and xenon.

Boeschoten and Van der Held [12] used helium, hydrogen and air at pressures from zero to atmospheric.

A general method of correlation has been suggested for gaseous conductance. This has been applied to the results of several investigations, covering a wide range of gases, types of surface, interface temperatures and gas pressures. Considering the inaccuracies inherent in this type of measurement, good correlation has been obtained. Most of the previous work has been carried out under conditions where the accommodation effect of gases is not important. The present work provides an extension to the region where the gap becomes comparable with the "accommodation length". The correlation of the gaseous conduction results is given by equation (13).

REFERENCES

1. R. HOLM, *Electric Contacts Handbook*, 3rd Ed. Springer-Verlag (1958).
2. F. P. BOWDEN and D. TABOR. *The Friction and Lubrication of Solids*. Clarendon Press, Oxford (1954).
3. R. A. PUTNAERGLIS, A review of literature on heat transfer between metals in contact and by means of liquid metals. Report No. R. 34, Department of Mechanical Engineering, McGill University, Montreal (1953).
4. T. N. ÇETINKALE and M. FISHENDEN, Thermal conductance of metal surfaces in contact. General discussion on heat transfer, *Instn. Mech. Engrs., Lond.* pp. 271–275 (1951).
5. H. FENECH and W. M. ROHSENOW, Thermal conductance of metallic surfaces in contact. U.S. Atomic Energy Commission, Report NYO-2136 (1959).
6. L. C. LAMING, Thermal conductance of machined metal contacts. International developments in heat transfer, *Amer. Soc. Mech. Engrs.*, 65–76 (1961).
7. F. P. BOWDEN and D. TABOR, The area of contact between stationary and between moving surfaces. *Proc. Roy. Soc.* A, **169**, 391–413 (1939).
8. E. H. KENNARD, *Kinetic Theory of Gases*. McGraw-Hill (1933).
9. T. N. ÇETINKALE, Thermal conductance of metal surfaces in contact. Ph.D. Thesis, London University (1951).
10. I. COHEN, B. LUSTMAN and J. D. EICHENBERG, Measurement of the thermal conductivity of metal-clad uranium oxide rods during irradiation. Report WAPD-228, U.S. Atomic Energy Commission (1960).
11. A. M. ROSS and R. L. STOUTE, Heat transfer coefficient between UO_2 and zircaloy 2. Report CRFD 1075, Atomic Energy of Canada Limited (1962).
12. F. BOESCHOTEN and E. F. M. VAN DER HELD, The thermal conductance of contacts between aluminium and other metals, *Physica*, **23**, 37–44 (1957).
13. V. C. HOWARD and T. F. GULVIN, Thermal conductivity determinations on uranium dioxide by a radial flow method. IG Report 51 (RD/C) (1961).
14. D. TABOR, *The Hardness of Metals*. Clarendon Press, Oxford (1951).
15. R. HILL, *Plasticity*. Clarendon Press, Oxford (1950).

APPENDIX

Indentation hardness

It is usual to estimate the actual area of contact from equation (3).

The use of the value of indentation hardness as normally measured is only valid for a limited range of conditions. To examine these limitations in detail would require a discussion of the plastic properties and theory of deformation of materials beyond the scope of the present work. A brief outline only of the points to be considered is given below. For the detailed background the reader is referred to one of the standard books on the subject, e.g. Hill [15], and for the specific application to hardness to Tabor [14].

The most important characteristic of a material which is being plastically deformed is its resistance to deformation. A convenient measure of this is its flow stress, σ, under simple uniaxial stress—the same value in tension or compression for an ideal plastic material. The commonest measure of hardness is the contact pressure between the material and a blunt, pyramid, cone or ball, indenter. It is found that, provided the material is homogeneous and initially stress free and the specimen sufficiently large, the indentation hardness is always very nearly 3σ.

Three properties of real materials may invalidate the use of this value of hardness, inhomogeneity, creep, and work hardened surface layers, the effects becoming relatively more important as the size of the indentation is reduced.

The effective indentation hardness will also be influenced by any stresses in the material around the indentation additional to those due to the indenter itself. Two cases are important for the present discussion:

(a) Stresses due to adjacent indenters will in general reduce the effective indentation hardness. The most important factors influencing this reduction are the ratio r_e/r_c, the ratio of the thickness to the width of the body of the material which is being made to flow, the rate of work hardening, and the friction between the surfaces. If either the friction is small enough or the thickness-to-width ratio large enough, the average compressive stress in the body of the material cannot exceed σ, i.e. as contact over the total area is approached, the effective indentation hardness drops from 3σ to σ.

(b) Transverse stresses in the surface. For the present discussion the Tresca yield condition is assumed to represent the plastic behaviour of materials sufficiently accurately. This states that the material will flow when the modulus of any shear stress exceeds $\sigma/2$. Consider an indentation stress of σ_x, i.e. a pressure of $-\sigma_x$, applied to a surface which has principal stresses σ_y and σ_z in the plane of the surface. If $\sigma_x < \sigma_z < \sigma_y$, the yield criterion is $\sigma_x = \sigma_y - \sigma$.

Of particular interest is the expansion of one cylinder inside another. If the radius of the interface is r and the outer cylinder has a wall thickness s, the elastic stresses ratios are:

$$\frac{s}{r} \ll 1, \frac{\sigma_y}{\sigma_x} = -\frac{r}{s};$$

yielding occurs when $\sigma_x \simeq -\frac{s}{r}\sigma$,

$$\frac{s}{r} \to \infty, \frac{\sigma_y}{\sigma_x} \to -1;$$

yielding occurs when $\sigma_x = -\frac{\sigma}{2}$.

This shows that complete contact will be obtained at a contact pressure of one sixth of the normal indentation hardness for a thick-walled cylinder and at much lower values for thin-walled cylinders. Contact sufficient to give very high values of solid conductance will be obtained at even lower values of contact pressure. This explains the observations of Cohen, Lustman and Eichenberg [10].

On reducing p from a maximum value $\hat{p}$ the contact area will be reduced. Bowden and Tabor [7] use the Hertz theory of elastic contact of spheres to deduce the expression, reproduced by Çetinkale and Fishenden [4]:

$$\frac{a_e}{a_\theta} = \frac{\hat{p}^{1/3}p^{2/3}}{3\sigma}. \tag{14}$$

This assumes that the elastic stress system behind a contact is very similar to that in a sphere of a diameter which gives the same contact area for the contact load. This will not be the case when the plastic zone has extended an appreciable distance into the material. To take the limiting case of full contact, the stress system is simple compression. On reducing load, full contact would be expected to be maintained, even down to zero load. In practice very small relative movement due to vibration etc. of the surfaces restores the conditions of equation (3). Holm [1] quotes full contact being maintained down to $0.06\ \sigma$ when the specimens have polished surfaces and small relative movements are prevented.

Résumé—On a étudié la conduction thermique aux interfaces bioxyde d'uranium/acier inoxydable dans un appareil du type disque, sous vide et avec différents gaz à l'interface (helium, argon, néon), pour les domaines suivants des différents facteurs: rugosité de la surface: 11–1417 . 10^{-6} cm, hauteur moyenne arithmétique, mesurée par un analyseur Talysurf—pression du gaz à l'interface: 7–1226 mm Hg—pression de contact: 0–570 lb/in²—température moyenne à l'interface: 55–410°C—flux de chaleur: 1–55 cal/s.cm².

Afin d'obtenir des résultats cohérents, les surfaces de contact des échantillons de 2 cm de diamètre, étaient d'abord rendues optiquement planes, puis rugueuses de façon bien déterminée. La conductibilité thermique est la somme de la conductibilité solide par les petites surfaces de contact et de la conductibilité par la gaz à l'interface (le rayonnement est négligeable). Les valeurs expérimentales obtenues pour la conductibilité par le solide sont du même ordre que celles prévues par la théorie de Çetinkale et Fishenden. On a trouvé, comme prévu, que la conduction par voie solide entre le bioxyde d'uranium et l'acier inoxydable était très faible en raison de la dureté des matériaux et de la faible conductibilité thermique du bioxyde d'uranium.

Les valeurs de la conduction par le gaz, calculées d'après des modèles géométriques simples de la rugosité, et en tenant compte des effets d'accommodation lors des collisions entre les molécules de gaz et les surfaces, ont été comparées aux résultats expérimentaux actuels et à d'autres données publiées. Dans la presque totalité des cas, la conductibilité mesurée est dans un rapport inférieur à 2 avec la valeur calculée, ce que l'on considère comme un bon accord, étant donné le très grand domaine de variation des paramètres couvert par les expériences et l'imprécision inhérente à ce type de mesures.

Zusammenfassung—Die Wärmeleitung durch die Berührungsfläche Uranⁱⁱⁱⁱⁱoxyd/rostfreier Stahl wurde in einer Scheibenapparatur untersucht, sowohl unter Vakuum als auch mit verschⁱⁱⁱⁱᵉdenen Zwischengasen (Helium, Argon, Neon). Variiert wurden: die Rauhigkeit (11–1417) × 10^{-6} cm, als arithmetisch gemittelte Höhe aus Talysurf Profilkurven ausgemessen; der Druck des Zwischengases (7–1226 mm Hg); der Anpressdruck (0–40 kp/cm²); die mittlere Zwischentemperatur (55–410°C) und die Wärmestromdichte (1–23 W/cm²). Um konsiⁱtente Ergebnisse zu erreichen, wurden die Kontaktflächen der Probestücke vom Durchmesser 2 cm optisch eben geläppt und dann auf den vorgeschriebenen Betrag angerauht. Die Wärmeleitfähigkeit ergibt sich als Summe der Leitfähigkeit der Festkörper an den kleinen, unmittelbaren Berührungsstellen und der Leitfähigkeit des Gases in der Zwischenschicht (der Beitrag der Wärmestrahlung ist vernachlässigbar). Die Versuchsergebnisse für die Leitfähigkeit der Festkörper waren von gleicher Grössenordnung wie die nach der Theorie von Çetinkale und Fishenden ermittelten Werte. Wie erwartet erwies sich der Anteil der Festkörperleitung zwischen Urandioxyd und rostfreiem Stahl als sehr gering wegen der Härte der Materialien und der kleinen Wärmeleitfähigkeit des Urandioxyds.

Berechnete Werte der Leitfähigkeit des Gases basieren auf verschiedenen einfachen geometrischen Modellen für die Rauhigkeit unter Berücksichtigung von Akkomodationseffekten beim Aufprall der Gasmoleküle auf die Oberflächen. Diese Werte wurden mit vorliegenden Versuchsergebnissen und anderen Veröffentlichungen verglichen. In nahezu allen Fällen unterscheidet sich die gemessene Leitfähigkeit von der berechneten um weniger als den Faktor zwei, was als gute Übereinstimmung angesehen wird im Hinblick auf den grossen Bereich der betrachteten Variablen und die dem Messverfahren anhaftenden Ungenauigkeiten.

Аннотация—В вакуумной установке дискового типа исследовалась теплопроводность на границе раздела двуокиси урана и нержавеющей стали при наличии различных газов между поверхностями раздела (гелий, аргон, неон). Степень шероховатости поверхности изменялась в пределах (11–1417)×10^{-6} см (арифметически средняя высота, рассчитанная по показаниям профилометра), давление газа на границе раздела—от 7 до 1226 mm Hg, местное давление соприкосновения—от 0 до 570 фунт/кв.дюйм, средняя температура на границе раздела—от 55 до 410°С и цлотность теплового потока—от 1 до 5·5 кал/сек см². С целью получения последовательного ряда результатов соприкасающиеся поверхности образцов диаметром в 2 см оптически плоско шлифовались, а затем им придавалась соответствующая степень шероховатости. Искомая теплопроводность определялась по значениям теплопроводности твердого вещества в местах непосредственного соприкосновения и теплопроводности газа на границе раздела (влиянием теплового излучения пренебрегали ввиду малости). Экспериментальные данные по теплопроводности твердого вещества хорошо согласовывались с данными, рассчитанными Четинкале и Фишенденом. Как и предполагалось, теплопроводность

твердого вещества при непосредственном соприкосновении двуокиси урана и нержаве-
ющей стали была невелика благодаря значительной твёрдости веществ и плохой
теплопроводности двуокиси урана.

Расчётные значения теплопроводности газа, полученные для простейших форм
шероховатости и учитывающие эффекты аккомодации при ударах молекул газа о
поверхности, сравнивались с экспериментальными результатами данной работы и
других опубликованных работ, Почти во всех случаях экспериментальные и расчётные
значения не отличались друг от друга более чем в 2 раза. что считается хорошим
   согласованием ввиду большого диапазона переменных и неточностей измерения.